

Article

Coarse Dynamics for Coarse Modeling: An Example From Population Biology

Justin Bush ¹ and Konstantin Mischaikow ^{2,*}

¹ Department of Mathematics, Hill Center-Busch Campus, Rutgers, The State University of New Jersey, 110 Frelinghuysen Rd, Piscataway, NJ 08854, USA; E-Mail: bushjc@math.rutgers.edu

² Department of Mathematics and BioMaPS, Hill Center-Busch Campus, Rutgers, The State University of New Jersey, 110 Frelinghuysen Rd, Piscataway, NJ 08854, USA

* Author to whom correspondence should be addressed; E-Mail: mischaik@math.rutgers.edu.

Received: 23 March 2014; in revised form: 29 May 2014 / Accepted: 6 June 2014 /

Published: 19 June 2014

Abstract: Networks have become a popular way to concisely represent complex nonlinear systems where the interactions and parameters are imprecisely known. One challenge is how best to describe the associated dynamics, which can exhibit complicated behavior sensitive to small changes in parameters. A recently developed computational approach that we refer to as a database for dynamics provides a robust and mathematically rigorous description of global dynamics over large ranges of parameter space. To demonstrate the potential of this approach we consider two classical age-structured population models that share the same network diagram and have a similar nonlinear overcompensatory term, but nevertheless yield different patterns of qualitative behavior as a function of parameters. Using a generalization of these models we relate the different structure of the dynamics that are observed in the context of biologically relevant questions such as stable oscillations in populations, bistability, and permanence.

Keywords: database for dynamics; conley theory; population model

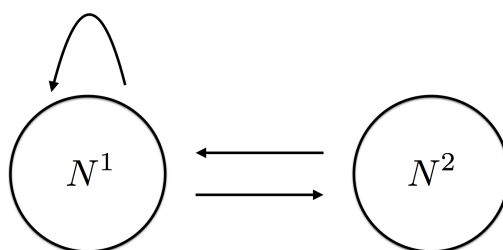
1. Introduction

Networks, in the form of directed graphs, have become ubiquitous as a modeling language for complex multiscale systems. In biological models the nodes of the graph are often used to denote species and a directed edge is used to indicate that one species directly affects another species. The usefulness

of the network language arises in part from the fact that, in the context of multiscale systems, species and, even more commonly, the interactions between the species are neither well defined nor understood. As an example, consider gene regulatory/signal transduction networks. In this case, the species are chemical compounds where the choice of which species and edges to include in a particular network is often based on statistical analysis. Nevertheless the purpose of the model is either to provide understanding of the experimentally observed dynamics or to provide a means of controlling the dynamics for engineering or health purposes.

As the work of the last century has demonstrated, the invariant structures of nonlinear systems can be extremely sensitive to arbitrarily small perturbations in the nonlinearities. For example, bifurcations can occur on a Cantor set in parameter space [1,2], making it hopeless to try to give an explicit account of the dynamics at every single parameter value. This suggests that the standard tools from nonlinear dynamics may not be adequate for the task of analyzing the potential dynamics of a system described in terms of a network. With this in mind, we have been developing a crude, but extremely robust, finite queryable representation of the global dynamics of multiparameter nonlinear systems that we refer to as a database for dynamics [3,4]. The philosophy of the database is that for many applications of dynamical systems—in particular ones where there is no reason to expect that parameters can be known with arbitrary precision—it is more meaningful to try to give an account of the dynamics valid for subsets of parameter space on the same scale that parameters can be measured. The mathematical starting point for the database is C. Conley’s approach to dynamics [5]. In particular, we make use of Morse decompositions as a means of decomposing the dynamics into gradient-like parts, and the Conley index as a means of rigorously identifying the structure of the recurrent dynamics. These ideas are discussed in Section 2.

The goal of this paper is to provide a concrete demonstration of the potential importance of this approach. This is done by considering a classical example from population biology: a nonoverlapping overcompensatory two age class model. From a network perspective this is an extremely simple system



where the first age class N^1 produces offspring (the self edge) and becomes the second age class N^2 , and the second age class produces offspring that belong to the first age class.

To explore the dynamics generated by models of this form requires choices of the population levels associated with the nodes and choices of the nonlinear interactions associated with the edges.

In Section 3 we provide justification for using the following map as an analytic representation for this network

$$\begin{aligned} N_{t+1}^1 &= \left(\sum_{i=1}^2 \theta_i N_t^i \right) e^{-0.1(\sum_{i=1}^2 (s\theta_{i+1}-s)N_t^i)} \\ N_{t+1}^2 &= 0.7N_t^1 \end{aligned} \quad (1)$$

For the moment we remark that it is obtained by generalizing the models considered in [6,7] and that there are three parameters; $0 \leq \theta_i, i = 1, 2$ which represent reproduction rates and $0 \leq s \leq 1$ which characterizes competition between age classes.

In light of our earlier comments, the purpose of exploring the dynamics is either to verify that this is an adequate model or, having accepted the validity of this model, to understand the expected observed behavior if parameters are changed. Several related observations are relevant at this point. First, Equation (1) makes use of the Ricker nonlinearity [8] which is unimodal, and thus it is reasonable to expect a period doubling cascade and the existence of infinitely many bifurcations on arbitrarily small scales with respect to parameters. Second, except for carefully controlled laboratory settings [9], population measurements are typically inaccurate and are subject to significant random perturbations. Thus, from an experimental perspective detecting the occurrence of bifurcations is at best nontrivial, which in turn calls into question whether one should attach theoretical significance to these bifurcations. Finally, the ‘verifiability’ of the different parameters are not the same.

For the moment it is sufficient to remark that we imagine that the reproductive rates, represented by θ_i , are more easily quantified than the degree or mechanisms of inter- and intra-species competition that we are modeling by s . In Section 3 we provide a rationale for the use of s as a parameter to model competition, but to a large extent it is based on ignorance. In light of the sensitivity of the structure of invariant sets in unimodal maps to small perturbations in parameters, detailed analysis of these structures seems irrelevant given the crude level of modeling employed.

With these observations in mind the goals of this paper are twofold: explain how the database technique can provide robust, but rigorous information about important dynamical structures, and at the same time demonstrate that intra-species competition plays a crucial role in determining the expected observable dynamics and, perhaps more significantly, has an important impact on the relative roles of the reproduction rates in achieving these dynamics. We provide a brief description of the database representation of the dynamics in Section 2. The complete results of performing the database computations on Equation (1) can be accessed at [10]. In Section 4 we use a subset of these results to discuss three biologically relevant issues:

- (1) biennial population dynamics,
- (2) bistability, and
- (3) permanence or persistence,

where we focus on how the choice of model, *i.e.*, the value of s , influences the relative significance of the reproduction rates θ_i .

2. Database of Dynamics

We provide a minimal review of the database approach to dynamics and refer the reader to [3,4] for more complete descriptions. Given a discrete-time dynamical system generated by a continuous function

$$f: \mathbb{R}^n \times \mathbb{R}^m \rightarrow \mathbb{R}^n$$

$$(x, z) \mapsto f_z(x) := f(x, z)$$

we are interested in a rigorous finite representation of the dynamics on a compact subset $X \subset \mathbb{R}^n$ of phase space over a compact set of parameter values $Z \subset \mathbb{R}^m$.

The first step in the computation of the database is a choice of discretization of X and Z . This is done by choosing a *grid* on both phase space and parameter space as defined in [11]. For the purposes of this paper we restrict ourselves to considering cubical grids, *i.e.*, a collection of closed cubes with nonempty interiors covering the space we are discretizing (either X or Z) such that distinct cubes may only intersect on their boundaries. In a scientific application the lengths of the edges of the cubes can be chosen in accordance with the scale on which reliable measurements can be made with respect to the variables and parameters. Let \mathcal{X} and \mathcal{Z} denote the grids for X and Z , respectively.

For each grid element of parameter space $\zeta \in \mathcal{Z}$ we construct a discretization of the dynamics. A convenient way of representing this discretization is with a set-valued function assigning to each $\xi \in \mathcal{X}$ a subset $\mathcal{F}_\zeta(\xi)$ of \mathcal{X} that reflects the underlying dynamics. We represent this set-valued function, which we call a *combinatorial multivalued map*, using the notation $\mathcal{F}_\zeta: \mathcal{X} \rightrightarrows \mathcal{X}$. The only essential requirement for making a rigorous statement about the dynamics using the Conley index, which we introduce shortly, is that \mathcal{F}_ζ be an *outer approximation* of f over ζ . Using $\text{int}(\cdot)$ to indicate the interior of a set, we say \mathcal{F}_ζ is an outer approximation if

$$f(\xi, \zeta) \subset \text{int}(\mathcal{F}_\zeta(\xi)) \quad \text{for all } \xi \in \mathcal{X}. \quad (2)$$

The map \mathcal{F}_ζ is not uniquely determined by this requirement and will depend on the numerical algorithms used to compute the image of f . Moreover, different outer approximations will potentially yield different qualitative information stored in the database. Indeed, as an extreme example one can check that the multivalued map sending every grid element ξ to all of \mathcal{X} satisfies the conditions of an outer approximation. Unsurprisingly, taking this as an outer approximation provides no useful information about the dynamics. We do not want to insist on a minimal outer approximation, however, because in general the cost of computation will be prohibitive. It is part of the power of the database approach to dynamics that we can make rigorous statements with any outer approximation, though it remains true that better outer approximations can give us a more refined picture of the dynamics.

Observe that a combinatorial multivalued map is equivalent to a finite directed graph with vertices \mathcal{X} and directed edges (ξ, ξ') whenever $\xi' \in \mathcal{F}_\zeta(\xi)$. With this in mind, we refer to \mathcal{F}_ζ as a multivalued map or a directed graph, whichever is more convenient or intuitive given the situation. From the directed graph \mathcal{F}_ζ we identify recurrent behavior by the existence of maximal *strongly connected path components*, *i.e.*, maximal subsets of \mathcal{X} with a directed path between any two elements in the set (or a self-edge in the case of just a one-element set). We use the following terminology:

Definition 1. Let \mathcal{F}_ζ be a multivalued map representing an outer approximation of the dynamics of a map $f: X \times Z \rightarrow X$ over a grid element $\zeta \in Z$. A *Morse set* is a strongly connected path component

of \mathcal{F}_ζ . Let P_ζ be an index set for the Morse sets of \mathcal{F}_ζ . Then the *Morse decomposition* of \mathcal{F}_ζ is the set $\{\mathcal{M}_{\zeta(p)} \subset \mathcal{X} \mid p \in P_\zeta\}$

Furthermore, \mathcal{F}_ζ induces a partial order on P_ζ in the following way: $p_1 \leq p_2$ if and only if there is a directed path in the graph \mathcal{F}_ζ from a grid element in $\mathcal{M}_{\zeta(p_2)}$ to a grid element in $\mathcal{M}_{\zeta(p_1)}$. Any recurrent dynamics must occur in the Morse sets, while gradient-like, transient dynamics must move down with respect to the partial order. We represent the Morse decomposition of \mathcal{F}_ζ and its associated partial order by the *Morse graph* MG_ζ , which is the Hasse diagram for the poset (P_ζ, \leq) [12].

The computations described above are performed for all $\zeta \in \mathcal{Z}$. We want to be able to identify whether the dynamics captured over different regions of parameter space are similar or distinct. To do this given $\zeta, \zeta' \in \mathcal{Z}$ such that $\zeta \cap \zeta' \neq \emptyset$ we define the *clutching graph* $\mathcal{I}(\zeta, \zeta')$ to be the bipartite graph with vertices $P_\zeta \cup P_{\zeta'}$ and with edges

$$(p, q) \in P_\zeta \times P_{\zeta'} \quad \text{if and only if} \quad \mathcal{M}_\zeta(p) \cap \mathcal{M}_{\zeta'}(q) \neq \emptyset.$$

If this bipartite graph induces an order preserving isomorphism between the MG_ζ and $MG_{\zeta'}$, then we declare that MG_ζ and $MG_{\zeta'}$ belong to the same *continuation class*. Extending this relation by transitivity we obtain a partition of parameter space such that each equivalence class defines the set of parameter values that belong to the same continuation class.

We made the statement that any potential recurrent dynamics must occur within the Morse sets. What is lacking at this point is a mathematical guarantee that a given Morse set contains nontrivial recurrent dynamics. This is done using the Conley index, an algebraic topological invariant. A detailed account of the Conley Index is outside the scope of this paper, but we refer the interested reader to [13]. For the purposes of this paper, it suffices to (a) explain how we represent the Conley index; (b) state some basic theorems regarding the Conley index; and (c) explain the connection between the Conley index and the underlying recurrent dynamics we are interested in.

We begin with a fundamental definition and result.

Definition 2. A compact set $N \subset X$ is an *isolating neighborhood* under f_z if the maximal invariant set in N , denoted by $\text{Inv}(N, f_z)$, is contained in the interior of N , i.e.,

$$\text{Inv}(N, f_z) \subset \text{int}(N).$$

The following result is proven in [14]. If \mathcal{F}_ζ is an outer approximation of the dynamics of a map $f : X \times Z \rightarrow X$ over a grid element $\zeta \in Z$, then for every $z \in \zeta$, and for every $p \in P_\zeta$, $\mathcal{M}_\zeta(p)$ is an isolating neighborhood under f_z . The Conley index can be viewed as an algebraic topological invariant for isolated invariant sets or isolating neighborhoods: if two isolating neighborhoods have the same maximal invariant set, then they have the same Conley index. Therefore, in particular, there is a well defined Conley index that can be associated to any Morse set $\mathcal{M}_\zeta(p)$.

So far we have spoken of “the” Conley index, but in fact there are choices to be made. Because there exist efficient algorithms for computing homology and induced maps on homology using the combinatorial map \mathcal{F}_ζ [15] we make use of the homological Conley index. For the purposes of this paper we choose to perform all of the homology computations with the coefficient ring \mathbb{Z}_3 .

There are two reasons for this choice. First, \mathbb{Z}_3 is preferable to \mathbb{Z}_2 because it allows us to distinguish 1 and -1 . This distinction is important, for example, when looking at fixed points with one-dimensional unstable manifold. If the map restricted to the unstable manifold is orientation-preserving, meaning that points near the fixed point are mapped to the same side of the unstable manifold, this will be reflected by a 1 on the induced map in first homology. On the other hand, an orientation-reversing map on the unstable manifold, which appears in the presence of a period doubling bifurcation, will be reflected by a -1 on the induced map in first homology. In the case of \mathbb{Z}_2 coefficients, however, this distinction cannot be made.

Second, \mathbb{Z}_3 is a field. When computing homology with field coefficients, the homology groups are vector spaces, and induced maps on homology are linear transformations. This greatly simplifies the algebraic problem of determining the Conley index. In particular, the Conley index in this setting is equivalent to the problem of determining the canonical form of a linear transformation away from zero eigenvalues [4]. Over the rational numbers \mathbb{Q} , this amounts to determining the Jordan blocks (over \mathbb{C}) with nonzero eigenvalues. In principle, the Jordan form over \mathbb{Z}_3 can be computed by passing to the algebraic closure, but this is a technical complication we can avoid by instead using the rational canonical form [16]. An equivalent way of expressing the rational canonical form is by a set of polynomials called the invariant factors, and there is a simple transformation for producing the invariant factors that eliminates zero eigenvalues.

In the context of this paper, we are restricting our attention to dynamics in \mathbb{R}^2 and thus the Conley index consists of at most three nontrivial lists of polynomials. Having performed the computations for Equation (1) we note that each list contains at most a single nontrivial polynomial and thus we denote the Conley index of a Morse set \mathcal{M} by

$$Con(\mathcal{M}) = (\phi_0(x), \phi_1(x), \phi_2(x)).$$

We say the Conley index is trivial if $\phi_i(x)$ is trivial for all $i = 0, 1, 2$.

Table 1 provides a partial dictionary for the Conley index: the invariant set on the left gives rise to the Conley index on the right. However, having the Conley index on the right does not imply that that associated maximal invariant set is the invariant set on the left. For example, a degenerate fixed point has trivial Conley index like the empty set, so one cannot conclude that the dynamics are trivial just because the Conley index is. An even more dramatic example of this is the fact that the Conley index of the Smale horseshoe is trivial, despite being a highly complicated invariant set. This is not meant to imply, however, that one cannot use the Conley index to obtain understanding of the structure of the invariant sets. For example, if the $Con(\mathcal{M}_\zeta) = (x^T - 1, \text{trivial}, \text{trivial})$, then \mathcal{M} consists of T distinct components K_i , $i = 1, \dots, T$ and $f_z(K_i) \subset K_{i+1}$, where $K_{T+1} = K_1$, for all $z \in \zeta$. We refer to such a Morse set as a *stable T -cycle set*.

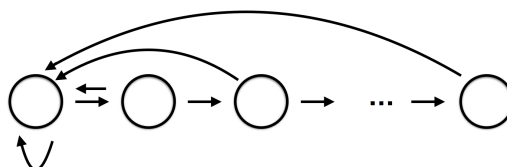
For each $\zeta \in \mathcal{Z}$, the associated *Conley-Morse graph* CMG_ζ consists of the Morse graph MG_ζ along with the Conley-index $Con(\mathcal{M}_\zeta(p))$ attached to the node $\mathcal{M}_\zeta(p)$. A fundamental result is that if two Morse graphs belong to the same continuation class, then they have the same Conley-Morse graphs.

Table 1. This table provides the Conley indices for elementary invariant sets. As discussed in the text, the converse does not hold, *i.e.*, the presence of a Conley index on the right does not imply the existence of the corresponding invariant set. All coefficients are mod 3.

Dictionary of Conley Indices	
Invariant Set	Conley Index (H_0, H_1, H_2)
\emptyset	(trivial, trivial, trivial)
stable fixed point	$(x - 1, \text{trivial}, \text{trivial})$
fixed point, 1-d unstable manifold, orientation preserving	(trivial, $x - 1$, trivial)
fixed point, 1-d unstable manifold, orientation reversing	(trivial, $x + 1$, trivial)
fixed point, 2-d unstable manifold, orientation preserving	(trivial, trivial, $x - 1$)
fixed point, 2-d unstable manifold, orientation reversing	(trivial, trivial, $x + 1$)
stable period- T orbit	$(x^T - 1, \text{trivial}, \text{trivial})$
period- T orbit, 1-d unstable manifold, orientation preserving	(trivial, $x^T - 1$, trivial)
period- T orbit, 1-d unstable manifold, orientation reversing	(trivial, $x^T + 1$, trivial)
period- T orbit, 2-d unstable manifold, orientation preserving	(trivial, trivial, $x^T - 1$)
period- T orbit, 2-d unstable manifold, orientation reversing	(trivial, trivial, $x^T + 1$)
stable invariant circle	$(x - 1, x - 1, \text{trivial})$
invariant circle, 1-d unstable manifold	(trivial, $x - 1, x - 1$)

3. Plant and Fish models

As indicated in the Introduction, the focus of this paper is on the database for dynamics as a tool in the modeling of complex systems where models cannot be completely determined from first principles. To make our discussion concrete we have chosen to work with an archetypical example, population biology. To keep the discussion as simple as possible we make use of discrete time models and consider the dynamics of the age-structured population of a single species. The network diagram for this type of system takes the form



indicating that with time each age class moves to an older age class and each age class produces offspring which become the youngest age class. While this network provides a framework in which to consider the problem, to understand the induced dynamics requires modeling assumptions concerning the edges/interactions. Most of what follows in this section is classical. However, we include it as it emphasizes the philosophy of how the database approach can be employed to identify sensitive aspects of the modeling process.

Let $N_{t+1} \in \mathbb{R}^n$ be the population vector representing the age structure of the population at time $t + 1$ where N_t^i denote the population of age class i . We assume that the future population is determined by a continuous function $N_{t+1} = f(N_t)$. The classical Leslie matrix provides a linear model [17], but fails to explain observed complicated population dynamics, and populations levels typically become extinct or unbounded. This suggests that a nonlinear function f may be a more appropriate choice. Certain biological assumptions will constrain the choice of f —for example in the absence of migration and abiogenesis, we want $f(0) = 0$. Furthermore, even in very simple models it is desirable to reflect the reality that a population cannot grow without bound. This can be accomplished by insisting for a sufficiently large population $|N|$ that $|f(N)| \leq |N|$.

There are many biologically plausible functions that meet these criteria [18]. A common way to ensure that the population remains bounded is to introduce an overcrowding effect that make the reproduction rates density-dependent in such a way that the reproduction rate grows more slowly for larger populations, perhaps even decreasing beyond a certain point.

One particular choice of unimodal nonlinearity for discrete time models is the Ricker nonlinearity [8], which in the simple case of only one age class N is given by

$$f(N) = Ne^{r(1-N/K)} \tag{3}$$

where the parameters r and K represents the growth rate for small populations and carrying capacity of the environment, respectively.

Depending on the kinds of data available to the ecologist, however, it may be more convenient to express this same nonlinearity using different parameters. Two standard reparameterizations are

$$f(N) = \theta Ne^{-bN} \tag{4}$$

(see [7]) and

$$f(N) = \theta Ne^{-b\theta N} \tag{5}$$

(see [6]).

Although these are just reparameterizations, they offer some advantages for interpretation. The parameter θ in each of these formulations, for example, represents the reproduction rate when the population is small and overcrowding effects are negligible. Perhaps more importantly, the exponent makes explicit what quantity is responsible for the overcrowding effect, whereby at sufficiently high populations the number of offspring actually decrease. Taking b to be a constant, in Equation (4) the exponent is proportional to the number of adults in the population, while in Equation (5) the exponent is proportional to the reproduction rate (in the absence of overcrowding) times the population.

Both Equations (4) and (5) can be extended to the case of multiple age classes (see [6,7]) following the approach of the Leslie matrix. This introduces parameters θ_i for the reproduction rate of age class i as well as ρ_i , the survival rate of the proportion of age class i to age class $i + 1$. In particular, Equation (4) generalizes to

$$N_{t+1}^1 = \left(\sum_{i=1}^k \theta_i N_t^i \right) e^{-b \sum_{i=1}^k N_t^i} \tag{6}$$

$$N_{t+1}^i = \rho_i N_t^{i-1} \quad i = 2, \dots, n$$

and Equation (5) generalizes to

$$N_{t+1}^1 = \left(\sum_{i=1}^k \theta_i N_t^i \right) e^{-b \sum_{i=1}^k \theta_i N_t^i} \quad (7)$$

$$N_{t+1}^i = \rho_i N_t^{i-1} \quad i = 2, \dots, n$$

As discussed above, each of these models can be given a different biological interpretation based on the exponent in the equation determining N_{t+1}^1 . Because the exponent in Equation (6) is proportional to the total population, this can be understood as representing the youngest members of the species being overcrowded by—or competing with—the existing adult population for resources. This might model, for example, the way that saplings compete with taller, more mature trees for sunlight. For this reason we will refer to Equation (6) as a “plant model”.

The plant model is discussed from a more classical point of view in [7] and from our database point of view in [3]. In particular, ([7], Figure 1) gives a picture of the bifurcation diagram along the line indicated in Figure 1. (Note that to make this comparison requires the choice of $\rho_2 = 0.7$.) The bifurcation diagram of [7] shows the presence of tremendously complicated changes in dynamics on fine scales that the database approach summarizes in a much coarser manner. In particular, the database reduces it to a relatively small number of Conley-Morse graphs.

In Equation (7), overcrowding depends on the potential number of recruits in the absence of any density-dependent effects. Holding the adult population constant and increasing the reproduction rate will increase the overcrowding in this model but not in the plant model. Biologically, this can be taken to represent the youngest members of the species being in competition with themselves. In [6] this is taken to be a model of a striped bass population, so for that reason we will refer to Equation (7) as a “fish model”.

We want to emphasize that both the fish and plant models have been extensively studied [6–8,18,19] and both models exhibit a *similar* wide range of dynamics: global stable equilibria, stable periodic dynamics, bistability, chaotic dynamics, etc. However, as indicated above these models are based on *different* assumptions concerning overcrowding. Furthermore, it is reasonable to suspect that in reality the youngest age group experiences competition *both* from themselves and from the older age groups. Thus a natural series of questions is the following:

Do the similarities observed in the dynamics of Equations (6) and (7) depend on the reproduction parameters in the same way? If so, can we understand this similarity in terms of the similar network structure of the two models? If not, can we understand the differences by putting these models in a wider context of models with the same network structure?

With this in mind it is natural to consider a possible continuum of intermediate cases where the young members of the species compete with both the adults and the offspring to different degrees. Since we have no explicit information about how this intermediate competition is taking place and since this competition is probably species dependent, the simplest way to realize this continuum is to take a linear interpolation between the two exponents using a new parameter $s \in [0, 1]$, *i.e.*,

$$\begin{aligned}
 N_{t+1}^1 &= \left(\sum_{i=1}^k \theta_i N_t^i \right) e^{-b(s \sum_{i=1}^k \theta_i N_t^i + (1-s) \sum_{i=1}^k N_t^i)} \\
 N_{t+1}^i &= \rho_i N_t^{i-1} \qquad i = 2, \dots, k
 \end{aligned}
 \tag{8}$$

This reduces to the plant model when $s = 0$ and the fish model with $s = 1$. In this larger framework we can observe how the dynamics change as the nature of competition changes by varying s .

Returning to the comments of the Introduction, given this crude level of modeling a detailed description of the dynamics on the level of invariant sets, especially given the complexity of this dynamics, appears unnecessary and, given the mathematical difficulty of obtaining such results, even counterproductive. In contrast, the database for global dynamics is based on dynamical information that can be extracted from outer approximations. The results of these computations are described in Section 4.

What should be noted at this point is that these results are based on the dynamics that can be extracted from the computed outer approximations \mathcal{F}_ζ . Assume that g is an alternative model to Equation (8) that is, for example, based on more information about the form of competition. Furthermore, assume that \mathcal{F}_ζ is an outer approximation for g , i.e.,

$$g(\xi, \zeta) \subset \text{int}(\mathcal{F}_\zeta(\xi))
 \tag{9}$$

(see Equation (2)), then the database information provided by the computations based on f are valid for g .

The obvious question is, how plausible is the assumption of Equation (9)? Since the computations we perform are based on rather crude grids in both phase and parameter space, and since we are using interval arithmetic to approximate the dynamics, we claim that this is not an unrealistic assumption. In particular, the computations could be performed at a lower resolution to gain further confidence in this assumption (see [10]).

4. Computational Results

In this section, we provide the results of the database of dynamics computations. Details about the algorithms we use are given in [4]. For the full database computation on the three parameters θ_1 , θ_2 , and s the reader is referred to [10]. This is a large data set. Thus, for the sake of clarity, we restrict our discussion to the following computations: the plant model Equation (6), the fish model Equation (7), and the mixed model Equation (8) at values of $s = 0.01, 0.02, 0.05$, and 0.1 . Again, the full output of these computations can be found at [10]. We limit our discussion to the effect of the choice of s on three typical biologically relevant questions.

We begin by discussing and justifying our choice of phase space X and parameter space Z . We then describe the database results for $s = 0$ (plant model) and $s = 1$ (fish model). This information is used to formally state the three questions of interest. We then discuss these questions based on the above mentioned computations of intermediate values of s .

Following [3,7] we restrict our computations to Equation (1) that is obtained from Equation (8) by restricting to two age classes and setting $\rho_1 = 0.7$. The parameter b is a scale parameter that has no effect on the dynamics, so we follow [3] and set $b = 0.1$. Even in this simplified setting the difference between the dynamics of the plant and fish models is apparent.

To perform the database computations we must restrict our parameter space to a compact set. Conceptually this is not a problem since there always exists an upper bound on the rate of reproduction, however appropriate values for this upper bound is a modeling question that is problem specific. Lacking this information, we have chosen to work with

$$Z = \{(\theta_1, \theta_2) \in [0, 50] \times [0, 50]\}$$

for various values of $s \in [0, 1]$, since this range of reproduction rates provides a diverse set of dynamics.

Similarly, the database computations require that we choose a compact phase space X . We note that Equation (1) has a global compact attractor and hence there exists a compact forward invariant region in $[0, \infty)^2$ that contains all the relevant dynamics. Explicit bounds on regions of this form this form depend on s and can be determined by bounding the number of new recruits:

$$N_{t+1}^1 = \left(\sum_{i=1}^k \theta_i N_t^i \right) e^{-b(s \sum_{i=1}^k \theta_i N_t^i + (1-s) \sum_{i=1}^k N_t^i)}.$$

The maximum of this function over the first quadrant is $\frac{10\bar{\theta}}{e(1+(\bar{\theta}-1)s)}$, where $\bar{\theta} = \max\{\theta_1, \theta_2\}$. This is a nondecreasing function of $\bar{\theta}$ for all $s \in [0, 1]$, so to determine a the maximum value for all choices of θ_1, θ_2 we set $\bar{\theta} = 50$. This gives an upper bound on the value of N_{t+1}^1 that also roughly corresponds to the scale of the dynamics. From this we can bound $N_{t+2}^2 = 0.7N_{t+1}^1$.

To allow for numerical error when computing the outer approximation, we round these values up when determining the size of phase space. For $s = 0$, for example, we take $X = [0, 200] \times [0, 140]$, while for $s = 1$ we take $X = [0, 5.0] \times [0, 3.5]$.

As we have emphasized, the scale at which X and Z are discretized into grids is an important consideration that will very much depend on the problem at hand. The precision with which the parameters can be measured, for example, gives one natural and meaningful choice of grid size. Because we are working with an abstract mathematical model in this paper, we have chosen the scale of our grids in phase and parameter space to best illustrate, given our computational resources, the change in dynamics between the plant and fish models. To this end, for each value of s we subdivide Z into a 128×128 parameter grid \mathcal{Z} . Similarly in phase space: for each value of s we use an adaptive grid described in [3,4] that is equivalent to a 4096×4096 grid \mathcal{X} on X . We further allow for additional subdivisions of Morse sets with trivial Conley index into smaller grid elements, to attempt to rule out numerical artifacts.

For each parameter grid element $\zeta \in \mathcal{Z}$, we must ensure the graph \mathcal{F}_ζ on \mathcal{X} is an outer approximation for the dynamics as described in Section 2. This can be accomplished with a variety of numerical techniques. We make use of the most straightforward approach, interval arithmetic. Details concerning the theory and implementation of interval arithmetic can be found in [20]. For our purposes it is sufficient to note that given a real valued function $r(a_1, \dots, a_k): \mathbb{R}^k \rightarrow \mathbb{R}$ and any assignment of intervals $[\underline{a}_i, \bar{a}_i] \subset \mathbb{R}$ to the variable $a_i, i = 1, \dots, k$, interval arithmetic returns an interval $[\underline{B}, \bar{B}]$ such that $r(\alpha_1, \dots, \alpha_k) \in [\underline{B}, \bar{B}]$ as long as $\alpha_i \in [\underline{a}_i, \bar{a}_i]$ for all i .

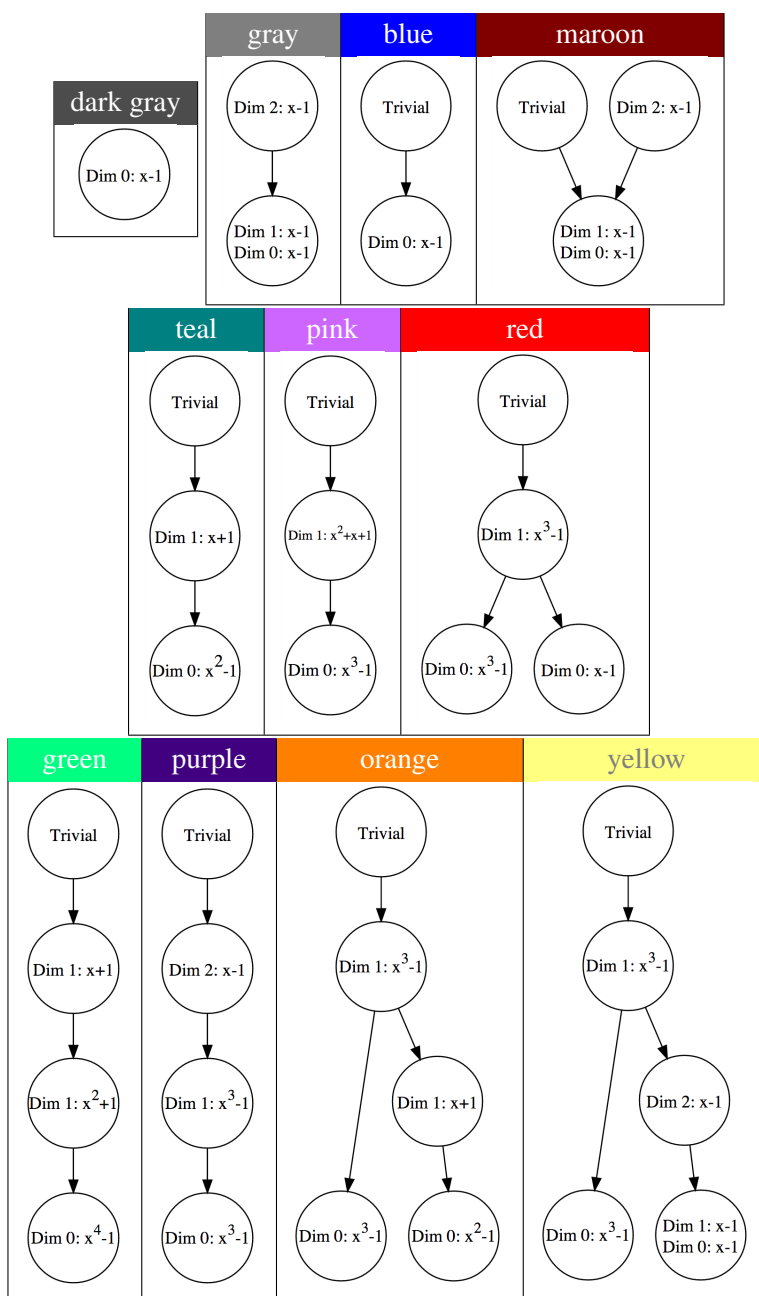
In order to compute the image $\mathcal{F}_\zeta(\xi)$ of a grid element $\xi \in \mathcal{X}$, we represent each parameter and phase variable as an interval using the intervals defining ζ and ξ , and then use interval arithmetic [20] to compute the image of the map. Note that the image is a rectangle in X . In general this rectangle will not

correspond precisely to a union of grid elements. Therefore, to ensure \mathcal{F}_ζ is an outer approximation we cover this rectangle by grid elements. For any grid element $\xi' \in \mathcal{X}$ that intersects this rectangle we add the edge $\xi \rightarrow \xi'$ to \mathcal{F}_ζ .

Turning to the discussion of the results of the database computations, we once again remind the reader that we are focusing on particular results. The full computations can be found at [10].

A description of eleven important Conley-Morse graphs, that arise in the computations mentioned above, is presented in Table 2. Each circle corresponds to a Morse set, and the directed edges between Morse sets indicate the partial order on the Morse sets as described in Section 2. Inside each circle are the polynomials constituting the Conley index for each Morse set computed with \mathbb{Z}_3 coefficients.

Table 2. Table of Conley-Morse graphs corresponding to each color



To obtain intuition about the dynamics associated with each Conley index we refer the reader to Table 1 and the discussion at the end of Section 2. Observe that there is a Morse set in the pink Conley-Morse graph with Conley index $x^2 + x + 1$ in dimension 1. This index does not appear in Table 1 so is worth an additional comment. The clutching graph stored in the database allows us to recognize this Morse set arises as the result of a Morse set with Conley index $x - 1$ in dimension 2 merging with a Morse set with Conley index $x^3 - 1$ in dimension 1. Thus we take as our representative dynamics an unstable fixed point with 2 unstable directions connecting to an unstable period 3 orbit with 1 unstable direction.

As indicated in Table 1, the Conley index of the empty set is trivial. However, as was discussed in Section 2 nontrivial invariant sets can also have trivial Conley index. In particular, for most of the parameter values being considered in this paper the origin is an unstable fixed point for Equation (1). However, because we are restricting the phase space to a compact subset of $[0, \infty)^2$, the Conley index of the origin is always trivial. This is explicitly seen in all the Conley-Morse graphs of Table 2 except for the Conley-Morse graph labeled gray and dark gray.

This has interesting implications, however, for the gray and dark gray Conley-Morse graphs. Namely, in these graphs our choice of outer approximation must not isolate the origin. In the case of the dark gray Conley-Morse graph, the fact that there is only one node implies that the computed isolating neighborhood for the globally stable dynamics in the interior of $[0, \infty)$ also contains the origin. Reviewing the full database results for the gray Conley-Morse graph leads to the same conclusion. Since in this biological system the origin plays the special role of extinction, this strongly suggests that for these parameter values stochastic perturbations can easily lead to extinction. We return to this discussion below.

Having established interpretations for the individual Conley-Morse graphs, we now turn to how they are related. Figure 1 displays a picture of parameter space output by the database for the plant model $s = 0$. Each color region indicates a subset of phase space with the same Conley-Morse graph. We hasten to add that this image represents a simplification of the continuation classes defined in Section 3. In particular, in Figure 1 the classification is based on purely on the Conley-Morse graph, ignoring the clutching graph information. This simplification is done for visual clarity; to see the complete continuation classes the reader is urged to download the database files and software from [10].

The major color regions in Figure 1 correspond to the labeling of Conley-Morse graphs in Table 2. Small changes in shading represent the presence of additional Morse sets with trivial Conley index in the Conley-Morse graph. As we have discussed, a trivial Conley index does not necessarily mean the invariant set of the underlying continuous dynamics is empty. Moreover, given our philosophy of working with the graph \mathcal{F}_ζ as a discrete representation of the dynamics on the parameter grid element ζ , we do not want to completely disregard the presence of Morse sets with trivial Conley index, since they can indicate recurrent behavior that is observed at the level of discretization chosen. There are two important mechanisms that lead to trivial Conley indices in these computations. The first is the presence of slow dynamics that numerically manifests itself as a kind of recurrent behavior. It should be noted that what is meant by “slow” will depend on the level of discretization. The second is the presence of invariant dynamics, the structure of which cannot be identified at the given level of resolution. In either

case the existence of a recurrent set with trivial Conley index is an indicator of a region in phase space to which additional attention may wish to be drawn.

Figure 1. Picture of parameter space for database computation with $s = 0$, *i.e.*, the plant model. As in all subsequent figures, the x -axis corresponds to θ_1 (young age class reproduction rate) and the y -axis θ_2 (old age class reproduction rate). The bold diagonal line corresponds to the bifurcation diagram in ([7], Figure 1). See Table 2 for the Conley-Morse graphs corresponding to each color.

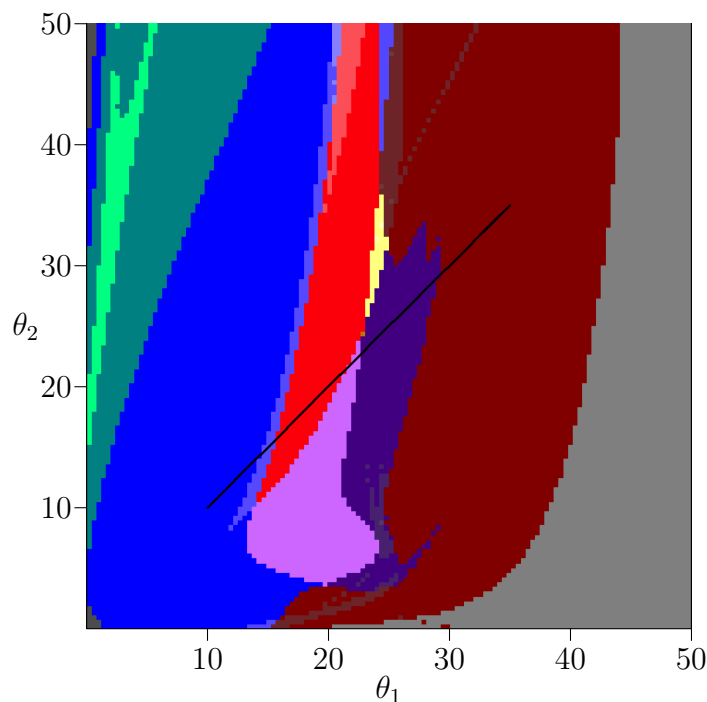


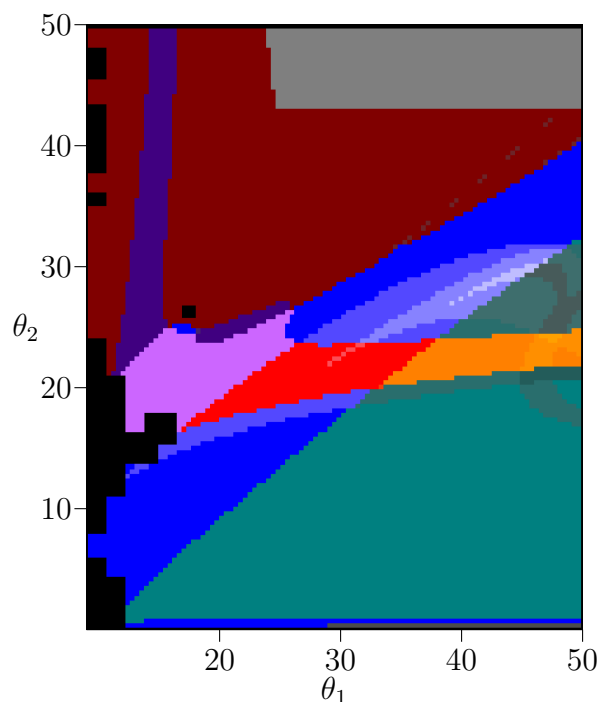
Figure 2 shows the same picture as Figure 1 except for the fish model $s = 1$. From the image alone we can see the answer to our question from Section 3: that despite sharing many of the same dynamics, the way that those dynamics are situated in parameter space is quite different between the plant and fish models. Thus, our objective now is to understand what connection, if any, there is between the similar dynamics as we vary the competition parameter s that interpolates between the two models.

To do the comparison we have chosen to focus on three distinct dynamical phenomena that have biological interest.

(1) Biennial Population Dynamics. The teal and green Conley-Morse graphs exhibited in Table 2 indicate the presence of stable 2-cycle sets and stable 4-cycle sets, respectively. Referring to Figure 1 for the plant model, the teal region is in the upper-left corner corresponding to small θ_1 and large θ_2 . Thus we can observe robust biennial behavior in the presence of a small amount of reproductive capacity by the younger age cohort.

In the corresponding figure for the fish model, Figure 2, the teal stable 2-cycle region is larger, but it is oriented along the θ_1 axis. Hence the dependence on stable biennial dynamics on the rates of reproduction appear to be opposite. An interesting question is if there is any connection between these two regions that can be observed in the intermediate models. In other words, as s is varied is there a choice of reproductive rates that preserves stable biennial population dynamics?

Figure 2. Picture of parameter space for database computation with $s = 1$, *i.e.*, the fish model. This is an image of the subset $[9, 50] \times [0, 50]$ of the full parameter space. The black regions along with the region $\theta_1 \leq 9$ were not computed due to memory constraints. See Table 2 for the Conley-Morse graphs corresponding to each color.



We remark that choosing a particular parameter value and examining the associated stable 2-cycle Morse sets in phase space shows that this biennial behavior corresponds to alternating high-low populations between the two age cohorts. Of course, the actual values, *i.e.*, location in phase space, is parameter dependent and thus not directly accessible from the database.

(2) *Bistability.* Bistability is easily detected in the Conley-Morse graphs; it occurs if there is more than one minimal node in the Conley-Morse graph. Thus, the red, orange, and yellow Conley-Morse graphs imply the existence of bistable dynamics. The dynamics within attractor can be identified via the Conley index. Thus, the red Conley-Morse graph indicates that one attractor is a stable 3-cycle set while the other attractor is a 1-cycle set. Referring to Figure 1 for the plant model, the red region is vertically oriented, so that it is sensitive to small changes in θ_1 but robust to changes in θ_2 . In the fish model, Figure 2, this is reversed, and the bistable region is much more sensitive to changes in θ_2 compared to θ_1 . As in the case of the biennial population dynamics, there is the question of whether these dynamics are related by the intermediate models.

Observe that in the fish model the teal region and the red region intersect in the region that is colored orange. As the orange Conley-Morse graph indicates this region exhibits characteristics of both the teal and the red regions—bistability where one attractor is a stable 3-cycle set and the a stable 2-cycle set. These dynamics are not detected by the database computations in the plant model.

(3) *Lack of Permanence.* We are using a continuous deterministic model of discrete populations, which is suspect for small population levels for at least two reasons: (i) the model can predict population levels

below a single unit; and (ii) when the origin is unstable the model does not allow a positive population to become extinct, a phenomenon that one would expect to occur due to stochastic perturbations. The concepts of permanence [21] and persistence [22], which in our setting is equivalent to the attractor of the positive orthant being bounded away from the origin, were introduced to address this concern. An advantage of the database approach is that it allows one to incorporate these ideas.

Suppose that the phase space grid is chosen at a scale to address concerns (i) and (ii). For example, suppose that the grid element containing the origin is large enough to both contain all points in phase space smaller than a single unit of population and all points that random perturbations might take to extinction within one time step. Then the fact that the database computations use an outer approximation guarantees that every Morse set not containing the origin is bounded away from the origin, and that any such Morse sets which are stable can be said to exhibit permanence. In this direction the database provides a proof of this fact.

On the other hand, if the origin is not isolated by its own Morse set—for example, if the only attractor contains the origin—then it suggests that at these scales permanence is not achieved. This could be an artifact due to the choice of a poor outer approximation that prevents the database from separating stable dynamics away from the origin. However, if this is an important modeling issue, then it can be resolved, at a computational cost, by using a better outer approximation to determine the multivalued map. And in every case the database indicates all regions of parameter space with possible lack of permanence.

As is discussed above, the origin is not isolated in the gray and dark gray Conley-Morse graphs. We focus on the gray Conley-Morse graph where the minimal Morse set has the Conley index associated with a stable invariant circle (see Table 1). In fact, the dynamics on the associated Morse set includes both the origin and large oscillations in the population. It is reasonable to expect due to stochastic fluctuations or population levels smaller than a single unit that extinction will occur.

As indicated in Figure 1 for the plant model the gray Conley-Morse graph occurs for large θ_1 , *i.e.*, if the first age class produces large numbers of seeds then extinction is expected. It is interesting to note that biennials typically produce no seeds the first year. Furthermore, for θ_1 sufficiently large, this phenomenon is essentially independent of θ_2 . Figure 2 shows that for the fish model again this dependency is reversed. Sufficiently high θ_2 given a moderate θ_1 means extinction, and these dynamics are relatively insensitive to θ_1 .

We are interested in understanding how these phenomena (biennial population dynamics, bistability and lack of permanence) depend upon the type of intra-species competition. Thus we perform the database computations using Equation (1) at the parameter values $s = 0.01, 0.02, 0.05,$ and 0.10 . To explain the nonuniform choice of s it should be noted that while s is taken to be a linear interpolation parameter between the exponents of the plant and fish models, it does not follow that the dynamics changes in a uniform manner. In fact, because for $\theta_i > 1$ the exponent in the fish model is larger than that of the plant model, the dynamics at $s = 0.1$ already begin to strongly resemble the dynamics of the fish model at $s = 1$.

Figures 3–6 identify regions of parameter space with the Conley-Morse graphs of Table 2 for the values $s = 0.01, 0.02, 0.05,$ and 0.10 , respectively. Looked at in sequence this gives a picture of how the dynamics over parameter space can be expected to change in response to a change in the nature of

competition. In particular, we revisit the contrasts observed between the dynamics of the plant and fish models to see how these phenomena behave over the transition.

Figure 3. Picture of parameter space for database computation with $s = 0.01$. See Table 2 for the Conley-Morse graphs corresponding to each color.

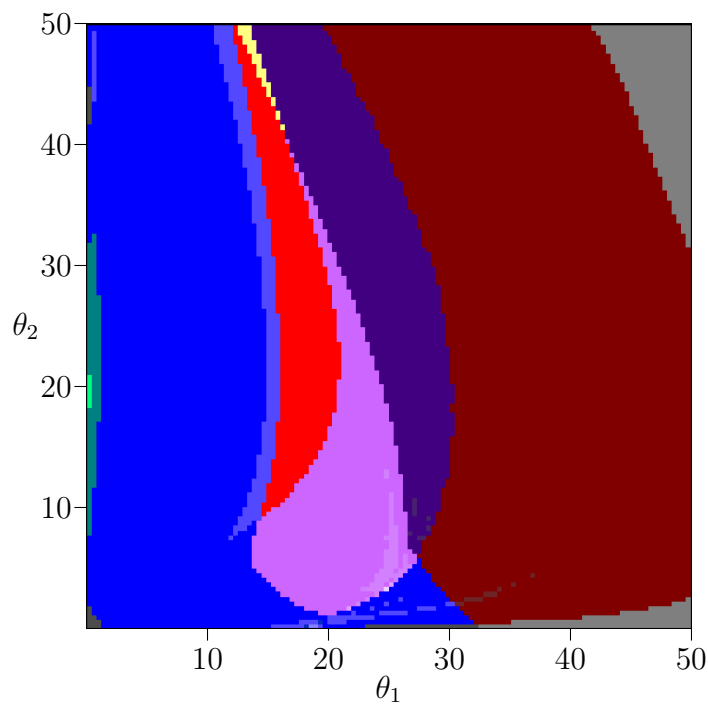


Figure 4. Picture of parameter space for database computation with $s = 0.02$. See Table 2 for the Conley-Morse graphs corresponding to each color.

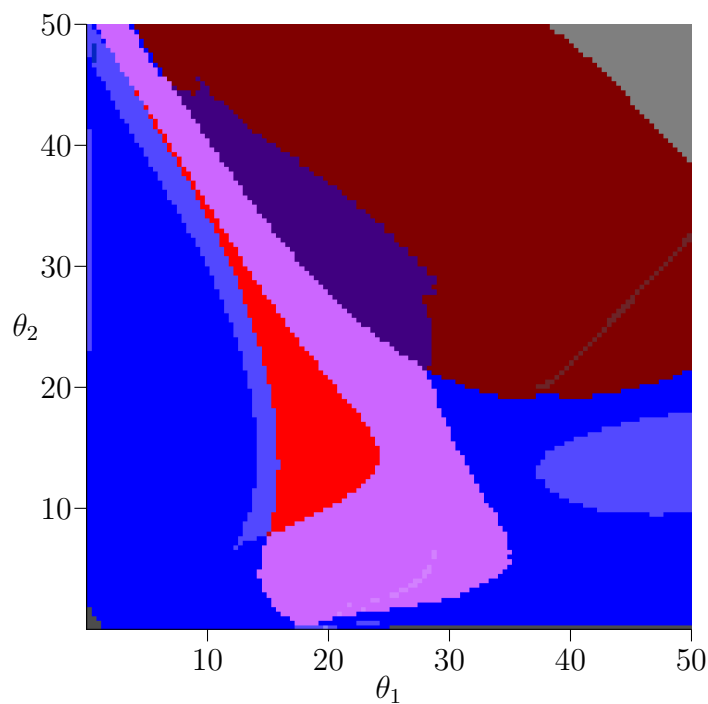


Figure 5. Picture of parameter space for database computation with $s = 0.05$. See Table 2 for the Conley-Morse graphs corresponding to each color.

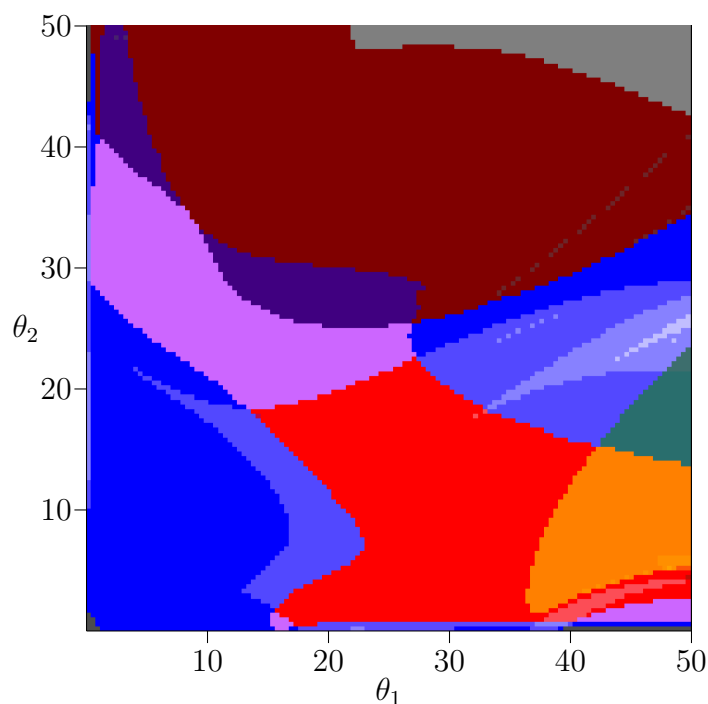
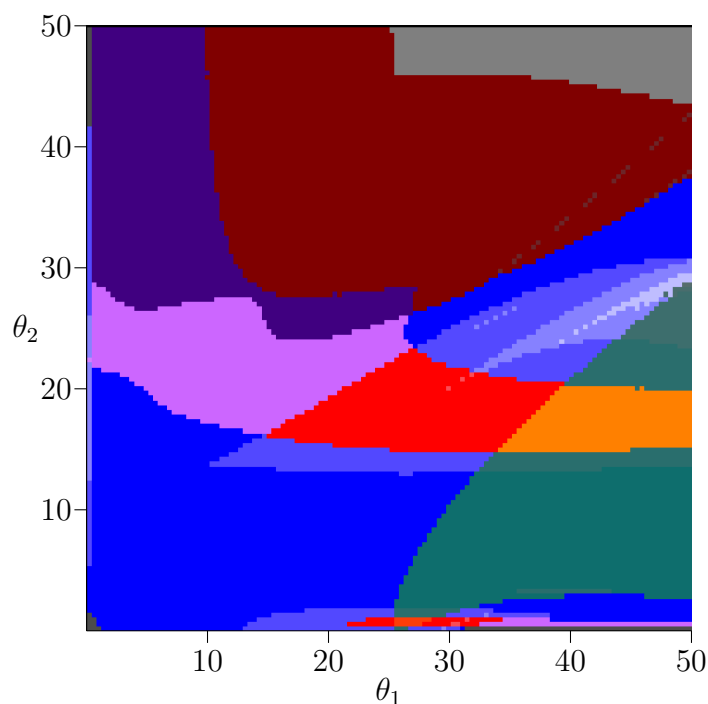


Figure 6. Picture of parameter space for database computation with $s = 0.1$. See Table 2 for the Conley-Morse graphs corresponding to each color.



(1) *Mixed Competition and Biennial Population Dynamics.* The teal Conley-Morse graph (Table 2) which indicates the existence of a stable 2-cycle and occupies most of the upper left corner of parameter space for the plant model (Figure 1) is already much less robust by $s = 0.01$ (Figure 3) and absent by

$s = 0.02$ (Figure 4). It reappears at $s = 0.05$ (Figure 5) for large values of θ_1 and moderate values of θ_2 . We can see that this 2-cycle region moves closer to the origin as s increases from 0.05 to 1 (Figures 5 and 6).

From this, we observe that the stable 2-cycle dynamics of the plant model do not appear to continue to the stable 2-cycle dynamics of the fish model. In other words, if the nature of competition changes within a biennial population from plant-like to fish-like, then there is a point at which the biennial dynamics will be lost, regardless of what happens to reproduction rates.

(2) *Mixed Competition and Bistability.* The red, orange, and yellow Conley-Morse graphs indicate the existence of bistable dynamics. These colors are present in Figures 3–6, which suggests that bistability persists under continuous changes in s . The ecological interpretation is that bistable dynamics is robust to changes in the type of competition experienced by the young members of the species.

Although bistability is present in each slice of parameter space, the shape of the bistable region changes with s . For $s < 0.05$ the region is more extended in the θ_2 direction, although by $s = 0.02$ the tail that extends primarily in the θ_2 direction is very narrow. By $s = 0.05$ things look quite different—the bistable region is much larger and extends much further along the θ_1 direction than the θ_2 direction. For $s = 0.1$ and $s = 1$ this orientation is preserved and the bistable region narrows further in the θ_2 direction.

(3) *Mixed Competition and Lack of Permanence.* While in the plant and fish models a lack of permanence (represented by the gray regions) could be reasonably described in terms of thresholds—large θ_1 in the plant model and a combination of large θ_2 and moderate θ_1 in the fish model—in the intermediate models this no longer holds. In the case of $s = 0.01$, for example, large values of θ_1 do not exhibit permanence if θ_2 is sufficiently large or small, but do exhibit permanence for moderate values of θ_2 . And even this non-monotone behavior is not described by a threshold: looking at the upper right corner when $s = 0.01$ or 0.02, there is a tradeoff between θ_1 and θ_2 that determines whether there is permanence, given by the slope of the boundary.

5. Conclusions

Typically, network diagrams are used to model complex systems in settings in which there is limited understanding of the specific mechanisms associated with the interactions. The standard expectation is that different modeling assumptions concerning these mechanisms will lead to different dynamics, and, in fact, for many models the structure of invariant sets are extremely sensitive to small perturbations. However, in the context of limited information it seems reasonable to expect that one is only interested in those dynamic structures that are robust with respect to models and/or parameters. In addition, for many applications the precision with which measurements can be taken also limits the dynamics that are observable. The database approach to dynamical systems gives us a rigorous way to investigate qualitative dynamics that are robust to these limitations of precision and/or modeling.

There are other approaches to modeling dynamical systems that aim to reflect this inherent uncertainty. As is alluded to in our discussion on permanence, the inclusion of stochasticity into a model

is a fairly common technique. How our approach compares with a stochastic dynamical system depends on the kind of noise that is being modeled.

In the case where it is important to include unbounded noise, any rigorous statement hoping to summarize the dynamics needs to allow for low probability events that, for example, can move systems between different basins of attractions. Invariant measures provide a means by which one can hope to describe such systems. At the moment we know of no method for relating the structure of the Conley-Morse graphs to invariant measure. Nevertheless, if we believe that the system that we are exploring has an underlying deterministic model for which the coarse features can be captured analytically, then database computations that indicate multiple basins of attraction over a set of parameter values might suggest that the associated invariant measure is not unimodal.

If the model incorporates bounded noise (in either phase or parameter space), then the database approach can be used to make rigorous statements. Observe that if the noise in the dynamical system is bounded, then this can be incorporated into the outer approximation when the dynamics is combinatorialized. Thus, if we take our model to be a deterministic map along with bounded noise, the database can be used to prove that there can be no trajectory between two basins of attraction of the deterministic system even in the presence of noise.

Finally, there is another interpretation of the database that is broader than merely investigating the underlying deterministic dynamics, but that also does not fit neatly into any stochastic model. We might call this the “ruler” interpretation. Suppose we have instruments capable of measuring either the state or parameters of a system with a certain precision, e.g., with a ruler we might be confident we can measure to the nearest millimeter. The database computation we perform is still valid even if the act of measurement disrupts the system, as long as the disruption does not alter the measured value. In other words, the computation we perform is valid even if the ruler changes the length of what we measure, just so long as it changes in a way that rounds to the same value. This is distinct from typical stochastic models of noise for a couple reasons. First and most importantly, there need be no assumption about the distribution of the perturbations introduced. Second, the types of noise permitted depend on the grid chosen—intuitively, points near the center of a grid element can be moved in any direction, whereas points near the boundary can only be moved very small distances in the direction of that boundary, but much larger distances away from the boundary.

This kind of investigation can have potentially important implications for the practice of modeling. To the extent that the qualitative dynamics is preserved over parameter space, we can conclude that the particular choice of model is less important than the general structure given by the network diagram. On the other hand, to the extent that we see important changes in the structure of dynamics over parameter space we can say that it is important to supplement the network diagram with further modeling assumptions, even though the dynamics of interest may be very coarse.

In the example of overcompensatory age-structured population models, we see that two classical approaches using the same form of nonlinearity can exhibit similar dynamics while having those dynamics situated quite differently in parameter space. The two different models already have different *a priori* justifications in terms of the biological understanding of competition. The database computations confirm that even looking at the dynamics on a coarse level we can distinguish between

the models, despite the fact they arise from the same network diagram, use the same nonlinearity and locally exhibit the same dynamic structures.

By embedding these models into a larger model that incorporates an additional parameter s representing intraspecies competition, we indicate how the database can be used to investigate empirically the relative importance and impact of the structure of competition. It should be emphasized that the parameter s is really an ordinal parameter—it is hard to assign any significance to particular values beyond their ordering and it is not clear how it could even be measured. However, the database can be used to organize/characterize the changes in the qualitative dynamics corresponding to different levels of competition. In principle, the associated database information could suggest experimental tests to determine positions along this scale.

Acknowledgments

This work was partially supported by NSF-DMS-0835621, 0915019, 1125174, AFOSR and DARPA. The authors thank Shaun Harker for valuable technical assistance with the database software.

Author Contributions

Conception and Design: Justin Bush, Konstantin Mischaikow. Performed computations: Justin Bush. Analyzed Data: Justin Bush, Konstantin Mischaikow. Wrote Paper: Justin Bush, Konstantin Mischaikow.

Conflicts of Interest

The authors declare no conflict of interest.

References

1. Newhouse, S.E. The abundance of wild hyperbolic sets and nonsmooth stable sets for diffeomorphisms. *Inst. Hautes Études Sci. Publ. Math.* **1979**, *50*, 101–151.
2. Newhouse, S.E. New phenomena associated with homoclinic tangencies. *Ergod. Theory Dyn. Syst.* **2004**, *24*, 1725–1738.
3. Arai, Z.; Kalies, W.; Kokubu, H.; Mischaikow, K.; Oka, H.; Pilarczyk, P. A database schema for the analysis of global dynamics of multiparameter systems. *SIAM J. Appl. Dyn. Syst.* **2009**, *8*, 757–789.
4. Bush, J.; Gameiro, M.; Harker, S.; Kokubu, H.; Mischaikow, K.; Obayashi, I.; Pilarczyk, P. Combinatorial-topological framework for the analysis of global dynamics. *Chaos* **2012**, *22*, 047508.
5. Conley, C. *Isolated Invariant Sets and the Morse Index*; AMS: Providence, RI, USA, 1978; Volume 38.
6. Levin, S.A.; Goodyear, C.P. Analysis of an age-structured fishery model. *J. Math. Biol.* **1980**, *9*, 245–274.

7. Ugarcovici, I.; Weiss, H. Chaotic dynamics of a nonlinear density dependent population model. *Nonlinearity* **2004**, *17*, 1689–1711.
8. Ricker, W.E. Stock and recruitment. *J. Fish. Res. Board. Can.* **1954**, *11*, 559–623.
9. Costantino, R.A.; Desharnais, R.F. Chaotic dynamics in an insect population. *Science* **1997**, *275*, 389–391.
10. Mischaikow, K. CHomP. Available online: http://chomp.rutgers.edu/Archives/Databases_for_the_Global_Dy (accessed on 19 May 2014).
11. Mrozek, M. An algorithmic approach to the conley index theory. *J. Dyn. Differ. Equ.* **1999**, *11*, 711–734.
12. Davey, B.A.; Priestley, H.A. *Introduction to Lattices and Order*; Cambridge University Press: Cambridge, UK, 2002.
13. Mischaikow, K.; Mrozek, M. Conley index. In *Handbook of Dynamical Systems*; Elsevier: Amsterdam, The Netherlands, 2002; Volume 2, pp. 393–460.
14. Kalies, W.D.; Mischaikow, K.; VanderVorst, R.C.A.M. An algorithmic approach to chain recurrence. *Found. Comput. Math.* **2005**, *5*, 409–449.
15. Harker, S.; Mischaikow, K.; Mrozek, M.; Nanda, V. Discrete morse theoretic algorithms for computing homology of complexes and maps. *Found. Comput. Math.* **2014**, *14*, 151–184.
16. Dummit, D.S.; Foote, R.M. *Abstract Algebra*, 3rd ed.; Wiley: Weinheim, Germany, 2004.
17. Leslie, P.H. The use of matrices in certain population mathematics. *Biometrika* **1945**, *33*, 183–212.
18. May, R.M.; Oster, G.F. Bifurcations and dynamic complexity in simple ecological models. *Am. Nat.* **1976**, *110*, 573–599.
19. Guckenheimer, J.; Oster, G.; Ipaktchi, A. The dynamics of density dependent population models. *J. Math. Biol.* **1977**, *4*, 101–147.
20. Moore, R.E. *Interval Analysis*; Prentice Hall, Inc.: Upper Saddle River, NJ, USA, 1966.
21. Hutson, V.; Schmitt, K. Permanence and the dynamics of biological systems. *Math. Biosci.* **1992**, *111*, 1–71.
22. Waltman, P. A brief survey of persistence in dynamical systems. In *Delay Differential Equations and Dynamical Systems (Claremont, CA, 1990)*; Springer: Berlin, Germany, 1991; Volume 1475, pp. 31–40.